Sinmez and Koca
Journal of Biological Engineering (2025) 19:1
36-024-00464-x

Journal of Biological Engineering

RESEARCH

Open Access

Synthesizing hybrid copper phosphate ($Cu_3(PO_4)_2$) nanoflowers using Cu^{+2} and shed snakeskin: antioxidant, antibacterial, anticancer, guaiacol, anionic, and cationic dye degradation properties

Cagri Caglar Sinmez[1*] and Fatih Doğan Koca[2]

Abstract

Background Synthesis of organic@inorganic hNFs is achieved by the coordination of organic compounds containing amine, amide, and diol groups with bivalent metals. The use of bio-extracts containing these functional groups instead of expensive organic inputs such as DNA, enzymes, and protein creates advantages in terms of cost and applicability. In this study, the application potentials (antioxidant, antibacterial, anticancer, guaiacol, anionic, and cationic dye degradation) of hybrid (organic@inorganic) nanoflowers (hNFs) synthesized with Cu^{+2} and snakeskin (SSS) were proposed.

Results Morphology, presence, and composition of elements of Cu and SSS-coordinated hNFs (Cu@SSS hNFs) were shown through FE-SEM–EDX spectroscopy. According to FE-SEM findings, hNFs synthesized with 0.5 ml and 1 ml extract have diameters of 12.81 and 3 µm, respectively. Diffraction peaks of hNFs determined by XRD were consistent with JCPDS Card 00–022 –0548. Cu@SSS NFs showed antioxidant properties depending on time through DPPH scavenging behavior (ability (R^2: 0.5612, IC_{50}: 2.07 mg/ml). Cu@SSS hNFs synthesized coordination of SSS and Cu degraded (75%) methylene blue at the highest pH 9 condition. However, hNFs highest degraded (68%) brilliant blue in an acidic PBS medium. hNFs oxidized guaiacol depending on exposure time. Cu@SSS hNFs demonstrated antibacterial properties towards Gram (-/ +) pathogen strains (MIC: 60 µg/ml). The catalytic and antimicrobial properties of hNFs were mentioned by the Fenton reaction. The cytotoxicity of Cu@SSS hNFs on the lung carcinoma (A549) cell line was shown to be concentration-dependent by the MTT test assay (IC_{50}: 56.4 µg/ml).

Conclusion As a result, Cu-based hNFs synthesized by using an organic waste (SSS) might be improved for environmental and biomedical applications.

Keywords Antimicrobial, Antioxidant, Catalytic activities, Copper nanoflowers, Fenton, Shed snakeskin

*Correspondence:
Cagri Caglar Sinmez
cagrisinmez@erciyes.edu.tr
[1] Department of History of Veterinary Medicine and Deontology, Faculty of Veterinary Medicine, Erciyes University, Kayseri, Türkiye
[2] Department of Aquatic Animals and Diseases, Faculty of Veterinary Medicine, Erciyes University, Kayseri, Türkiye

Introduction

Nanomaterials exhibit superior properties with their morphology and properties. For this reason, it has been among the popular topics of both and scientific industrial fields such as electronic, optical, magnetic, nano-radiotracer applications, biomedical fields, enzyme and

environmental applications [1–5]. Various metallic NPs, such as monometallic NP and bimetallic NP, are synthesized by different approaches (physical, biological, chemical)—advantageously against each other [6]. In recent years, the biological synthesis method, which is carried out with low cost and energy needs without using chemical reducing agents, has become one of the popular topics [7, 8]. Kiani et al. (2024) reported that ZnO NPs synthesized with *Lavandula stoechas* extract exhibited antioxidant, anticancer, antimicrobial, and catalytic activities and that ZnO NPs can be used in environmental applications [9]. Zare-Bidaki et al. (2023) reported that AgNPs synthesized with Petroselinum crispum extracts have antifungal, antioxidant, and anticancer properties [10]. It has been reported that Ag NPs synthesized with various biological extracts in particular have application potential in various fields [11, 12]. Barzegarparay et al. (2023) reported that selenium nanoparticles (Se NPs) synthesized with Crataegus monogyna extract exhibited antioxidant and anticancer activity [13]. In another study, researchers reported that palladium (Pd) NPs synthesized with four different plant extracts caused catalytic degradation of thiazine dye (methylene blue), azo dye (methyl orange), and alkaline dye (rhodamine B) [14]. Habib et al. (2022) determined the antimicrobial activities of silver (Ag) NPs synthesized with *Zanthoxylum armatum* extract [15].

Recently, various nanofibers, magnetic nanoparticles, nanoflowers, and carbon-containing nanostructures have been applied to enrich the stability and catalytic properties of enzymes [16–19]. Hybrid nanoflowers synthesized by hybridization of organic components containing amine and diol groups with bivalent inorganic components attract attention with their layered surfaces and porous structures. The first time, Zare et al. (2012) synthesized hNFs by hybridization of protein and inorganic Cu^{+2} inputs and declared that the hNFs obtained by enzyme immobilization exhibited improved activity and stability [20]. A hybrid form of organic and inorganic, hNFs have a flower-shaped and porous structure and they are functional as carriers in the immobilization of biomolecules such as enzymes [16]. The highest surface area (surface/volume) of hNFs gives them an effective loading capacity, enhanced catalytic activity, and high stability. Studies are being carried out on the synthesis and applications of hNFs with various organic components and bivalent ions. Demirbaş et al. (2023a) reported that Cu hNFs, which they synthesized with amino acids (glycine and phenylalanine), exhibited catalytic activity against guaiacol [21]. Chen et al. (2024) suggested that protein@Cu hNFs might be used as sensors for the reveal of pyridaben [22]. Koshy et al. (2024) declared that hNFs obtained by using protein (silk sericin) could be applied in ciprofloxacin (antibiotic) degradation [23]. According to another study, it exhibited catalytic activity against the neutral red dye of hNFs obtained via the coordination of DNA and the Cu^{+2} [24].

The synthesis of hNFs occurs by the coordination of amide, hydroxyl, or carboxyl groups of organic components and bivalent elements. The synthesis of hNFs by using plant and organic wastes containing these biomolecules instead of DNA, enzymes, and amino acids attracts attention because they are cheap and easy to synthesize [25, 26]. Anticancer activity of hNFs synthesized via coordination of *Tribulus terrestris* and bivalent ions (Cu (II), Zn (II), and Co (II)) against lung cancer (A549) cells was recorded [27]. Antimicrobial, antioxidant, and catalytic properties of Cu-based hNFs synthesized through Saffron (*Crocus sativus*), *Parazoanthus axinellae* (anemone), *Umbilicaria decussata* (lichen) and *Aspergillus terreus* (fungal) extracts are the trend studies of recent years [28–31]. According to a study by Altınkaynak et al. (2018), egg white and Cu coordinated hNFs exhibited peroxidase-like activity and decolorized Direct Blue dye by 76% [32].

In this study, the *Elaphe sauromates*, a non-poisonous snake species [33], was selected as an organic component to coordinate with Cu^{+2}. In a previous study, it was reported that shed of *E. sauromates* contains α-keratin, fragile β-keratin, and many proteins and peptides [34]. The proteins found in the shed snakeskin (SSS) used in this study can coordinate with Cu^{+2} with the amine groups included, making SSS a good candidate for hNF synthesis. Herein, we report for the first time the synthesis of hNFs at medium pH ranging from 5 to 9 by coordination with SSS (different concentration) and Cu(II). SSS was selected for the synthesis of hNFs due to the presence of amine-group containing proteins, which reduces hNF production. Furthermore, antioxidant, antimicrobial, anticancer, anionic, and cationic dye degradation and guaiacol oxidation properties of Cu@SSS hNFs were determinded.

Materials and methods

Synthesis of Cu@SSS hNFs

Ventral portions of SSS were obtained from *Elaphe sauromates* (Fig. 1) which were supplied by the Anatolian Wonderland Zoo, Kayseri, Türkiye Dr. Coşkun TEZ identified the shed snakeskins at Erciyes University Department of Zoology. $CuSO_4.5H_2O$ and SSS extract (10g/100ml dH_2O) at different concentrations (0.5 and 1 ml) were added into PBS buffer with different pHs (pH 5–9) [25]. Vortexed (for 1 min) solutions were held at room temperature for 3 days in a dark medium and were characterized after centrifugation (10.000 rpm for 20 min) and drying (70 °C).

Fig. 1 Images of SSS of *Elaphe sauromates*

Characterization of Cu@SSS hNFs

Morphologies, inorganic and organic components, and crystal structures of Cu@SSS hNFs were determined. FE-SEM (Zeiss Gemini 500) images were used to determine the morphologies of hNFs. The presence of inorganic components in their structures was determined by EDX (EDX- ZEISS GEMINI 500) analysis. The crystallinity of Cu@SSS hNFs was examined by using an XRD (Panalytical, Empyrean) diagram. The presence of organic components in their structure was revealed by FT-IR (PERKIN ELMER, 400) peaks.

Antioxidant activity of Cu@SSS hNFs

The antioxidant activity of Cu@SSS hNFs was detailed by determining absorbance changes due to oxidation of the model substrate DPPH (2,2-diphenyl-1picrylhydrazyl). Based on the literature [35], after adding increasing concentrations from 0.165 mg/ml to 10 mg/ml Cu@SSS hNFs to the DPPH solution (0.1 mM), the absorbance of the incubated (for 30 min, in dark room) solutions was read on the spectrophotometer at 517 nm. Blank readings were performed using the same volume of ethanol (99.5%) instead of the DPPH solution. Antioxidant activities of hNFs were calculated with the formula below.

$$\text{Scavenging activity (\%)} = [(\text{Abs}_C - (\text{Abs}_S - \text{Abs}_B)]/\text{Abs}_C \times 100$$

Abs_c = control: distilled water, Abs_S: sample, Abs_b = blank: ethanol (99.5%).

Guaiacol degradation ability of Cu@SSS hNFs

In order to observe the ability of Cu@SSS hNFs to oxidize guaiacol via its catalytic pathway, 1 ml each of H_2O_2 (22.5 mM), guaiacol (45 mM), 3×10^{-3} g Cu@SSS hNFs were transferred to test tubes containing PBS (1 ml, pH 6.8) and vortexed for 1 min, then centrifuged at 4000 rpm [26]. Absorbance changes against the blank solution (without Cu hNFs) were recorded with spectrophotometer readings at 470 nm.

Dye degradation property of Cu@SSS hNFs

Previous literature was applied to examine the capacity of Cu@SSS hNFs to degrade methylene blue (cationic) and brilliant blue (anionic) at different pHs [25]. For this purpose, 1 ml of dye was transferred to 10 mM, 50 ml PBS buffer at increasing pH (5, 7.4, and 9) containing H_2O_2 prepared and vortexed. The absorbance changes for methylene blue observed at 664 nm by spectrophotometric measurements of the solutions incubated in the dark were used in the formula below to determine the percentage of dye removal ability of NFs. Spectrophotometric readings were taken at 590 nm to determine degradation of brilliant dye.

$$[\text{Dye degradation (\%)} = [(\text{Abs}_0 - \text{Abs}_1) \text{ x } 100/\text{Abs}_0]$$

Abs_0 first absorbance value, Abs_1 last absorbance value.

Antimicrobial property of Cu@SSS hNFs

Gram + (*Staphylococcus aureus*) and Gram—(*Pseudomonas aeruginosa, Escherichia coli*) pathogenic bacteria were used as model microorganisms in this test. The method involving the microdilution technique was applied to evaluate the MIC values of Cu@SSS hNFs [26]. Two-fold dilutions of Cu@SSS hNFs (concentration from 4 µg/ml to 512 µg/ml) were transferred to Muller Hinton broth with 1×10^8 CFU/ml. After the tubes were kept at 37 °C (1 day), the MIC value was determined by considering the turbidity in the tubes. Negative and positive control tubes were adjusted without bacteria and only bacteria tubes, respectively. The test was triplicated.

Anticancer activity of Cu@SSS hNFs

MTT protocol was used to determine the cytotoxicity of Cu@SSS hNFs. Human lung carcinoma cell lines (A549 (ATCC)) were incubated at 37 °C (5% CO_2,) in DMEM (Dulbecco's Modified Eagle's Medium)/F12 K (containing 10% fetal bovine serum with 1% penicillin–streptomycin). Cu@SSS hNFs dissolved in distilled water were serially diluted (from 250 µg/ml to 1.9 µg/ml) and transferred to the plates containing the cell line (density:12.500 cells/well) for incubation (overnight). After the 96 well plates were incubated for 24 h, absorbance readings were taken with a spectrophotometer at 572 nm [27].

Results

Characterization of Cu@SSS hNFs

FE-SEM images of Cu@SSS hNFs formed in PBS (pH = 7.4) by using 0.5 and 1 ml extract as the organic component are given in Fig. 2a and b. In the presence

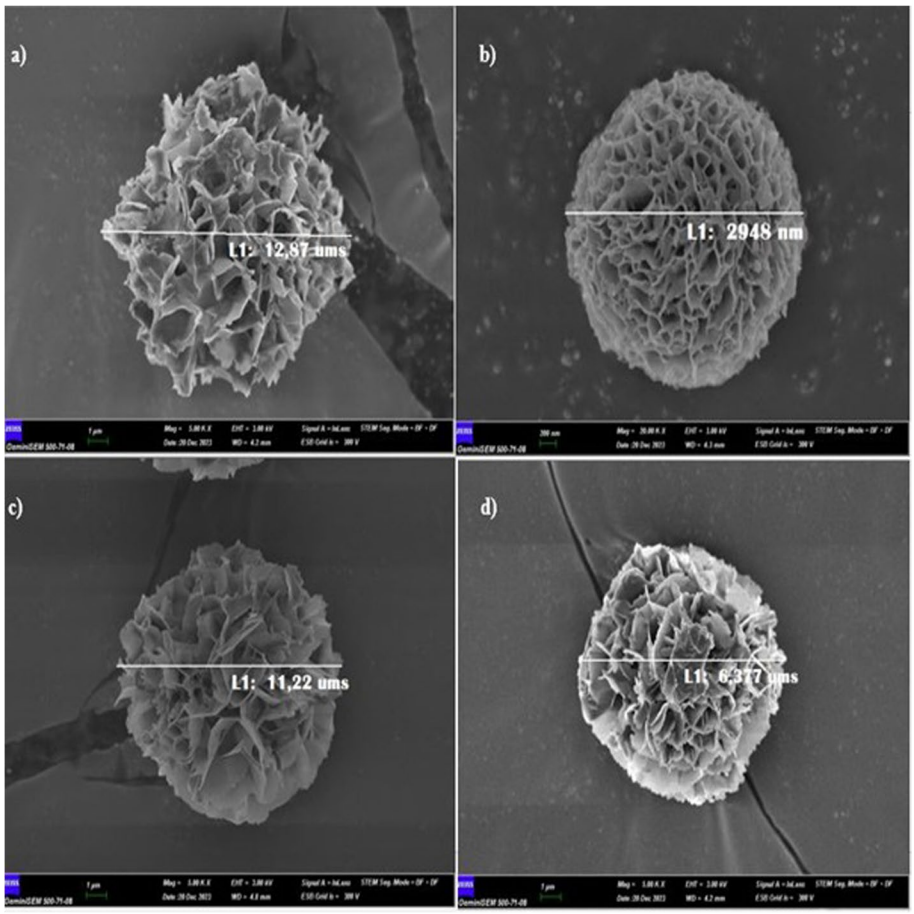

Fig. 2 FE-SEM images of Cu@SSS hNFs. **a** diameter of Cu@SSS hNFs synthesized at pH 7.4 with 0.5 ml SSS extract, **b** diameter of Cu@SSS hNFs syntheszied at pH 7.4, by using 1 ml SSS extract, **c** diameter of Cu@SSS hNFs synthesized at pH 9 by using 0.5 ml SSS extract, **d** diameter of Cu@SSS hNFs synthesized at pH 9 by using 1 ml SSS extract

of SSS at low concentration (0.5 ml), it was determined that the diameter of hNF was 12.81 µm, and the petals were loosely arranged and had a structure far from a full flower morphology. It was noted that hNF synthesized by increasing the concentration of SSS extract (1 ml) had a diameter of approximately 3 µm. Optimum synthesis of hNFs was achieved by coordination of 1 ml SSS extract and Cu^{+2} at pH 7.4 medium. The diameters of Cu@SSS hNFs obtained by using 0.5 and 1 ml of extract in alkaline PBS buffer were measured at 11 µm and 6 µm, respectively (Fig. 2c and d).

It was noted that the petals of hNFs synthesized with low concentration extract in alkaline medium had a loosely arranged structure, while at high concentration there were deteriorations in the petal and pore structures. hNFs synthesized under optimum conditions (PBS pH of 7.4, 1 ml extract) were used in characterization and other tests. Elemental composition of hNFs was revealed through the EDX diagram (Fig. 3). Through XRD analysis (Fig. 4), the peaks observed at $2\theta = 9°$, 13°, 18°, 20°, 24°, 30°, 34°, 37°, 41.52°, 45°, 54°, and 56°. Through FT-IR analysis, absorbances were recorded at 2926, 1621, 146, 1034, 986, 624, and 558 cm^{-1} (Fig. 5).

Antioxidant activity of Cu@SSS hNFs

The free radical (DPPH) scavenging efficiency of Cu@SSS hNFs with optimum morphology was examined spectroscopically. It has been detected that Cu@SSS hNFs exhibited DPPH scavenging ability ($R^2 = 0.5612$) depending on the concentration increase (Fig. 6). Our results show that the 2.07 mg/ml of Cu hNFs were required to scavenge 50% of DPPH.

Dye degradation activity of Cu@SSS hNFs

It was determined that hNFs (synthesized at pH 7.4, by using 1 ml extract) synthesized with SSS extract removed methylene blue, a cationic dye, at the statistically highest level at pH 9 (75%) and the lowest at pH 5 (44%) (Fig. 7a). Additionally, an increase in the degradation of methylene

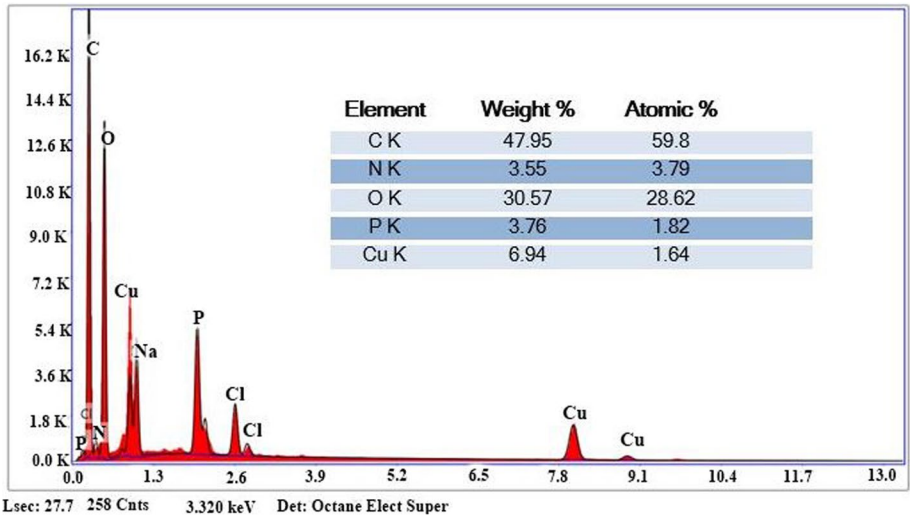

Element	Weight %	Atomic %
C K	47.95	59.8
N K	3.55	3.79
O K	30.57	28.62
P K	3.76	1.82
Cu K	6.94	1.64

Fig. 3 EDX analysis of Cu@SSS hNFs

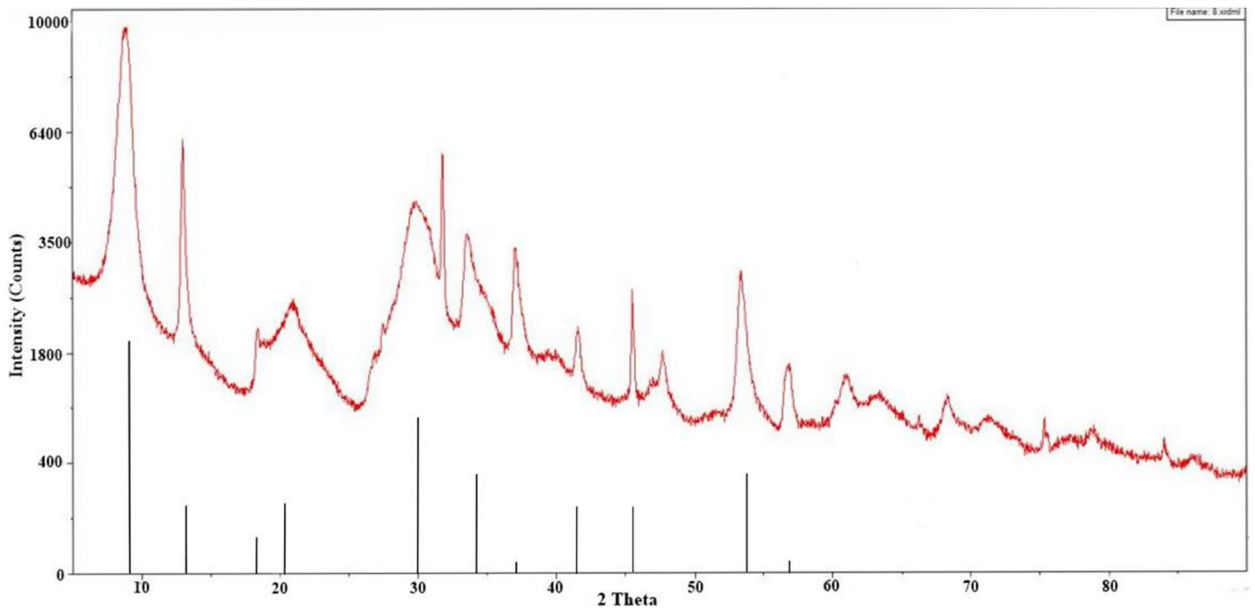

Fig. 4 XRD diagram of Cu@SSS hNFs. Black line indicates with JCPDS Card 00–022 –0548, red line indicates synthesized hNF

blue dye was observed with increasing time (Fig. 7b). The statistically highest degradation (68%) of brilliant blue was recorded in acidic (pH 5) PBS buffer (Fig. 8).

Oxidation of guaiacol by Cu@SSS hNFs

The ability of hNFs to degrade guaiocol through oxidation was recorded by spectrophotometric measurements. Depending on the exposure time, hNFs were determined to degrade guaiacol (Fig. 9). It was determined that the absorbance of guaiacol increased approximately 3 times from 0.075 nm to 0.235 nm.

Antimicrobial activity of Cu@SSS hNFs

In this study, the antimicrobial properties of Cu@SSS hNFs with optimum morphology were investigated against three Gram (-) and Gram (+) strains. The bacterial growth inhibitory activities caused by Cu@SSS hNFs were discussed by determining the MIC. The minimum inhibition concentrations of hNFs synthesized with SSS extract against *P. aeruginosa* and *E.coli* bacterial strains were identified at 30 µg/ml. For the *S. aureus* strain, the MIC was determined at 60 µg/ml.

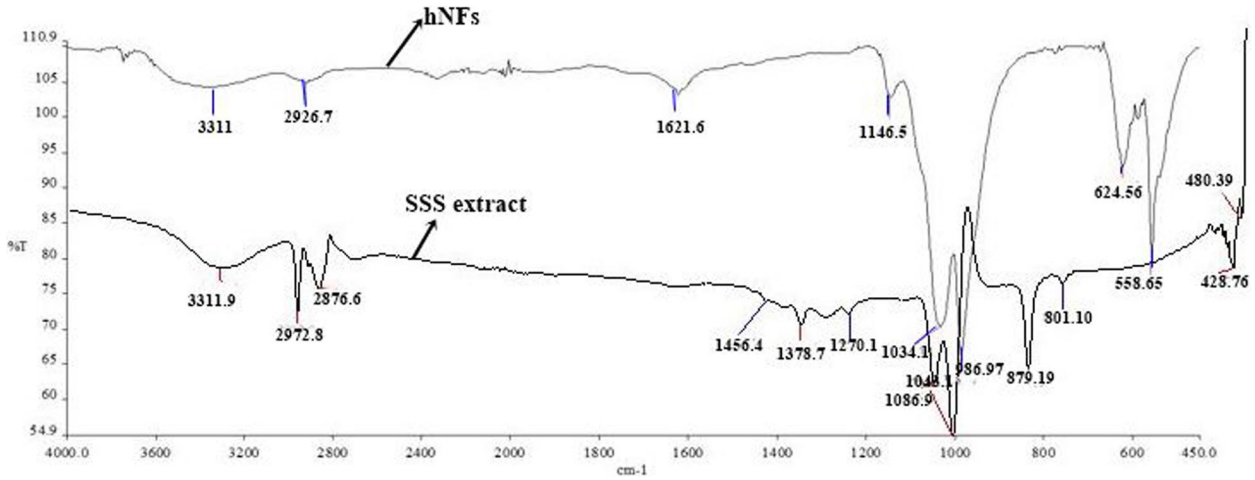

Fig. 5 FT-IR spectra of Cu@SSS hNFs

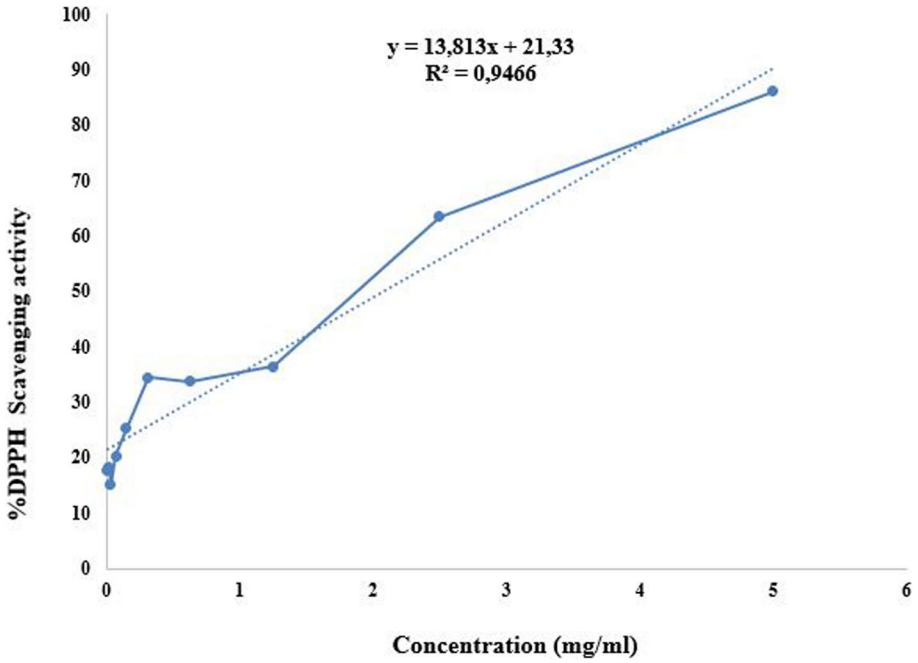

Fig. 6 Antioxidant activity of Cu@SSS hNFs

Anticancer activity of Cu@SSS hNFs

It was determined that exposure of A549 cells to Cu@SSS hNF caused loss of viability in the cell line (Fig. 10). Increasing concentrations of Cu@SSS hNFs (1.9–250 µg/ml) were applied to A549 cell lines, and a statistically significant decrease in cell viability was observed at 15.6 µg/ml concentration application. In this experiment, the IC_{50} of Cu@SSS hNFs against A549 cell lines was calculated as 56.4 µg/ml.

Statistical analysis

Data were evaluated using the IBM SPSS Statistics Standard Concurrent User V 29 (IBM Corp., Armonk, New York, USA) statistical package program. Descriptive statistics were given as mean ± standard deviation. The normal distribution of data belonging to numerical variables was evaluated using the Shapiro Wilk normality test. The homogeneity of variance of the groups was analyzed using the Levene test. The level of deterioration

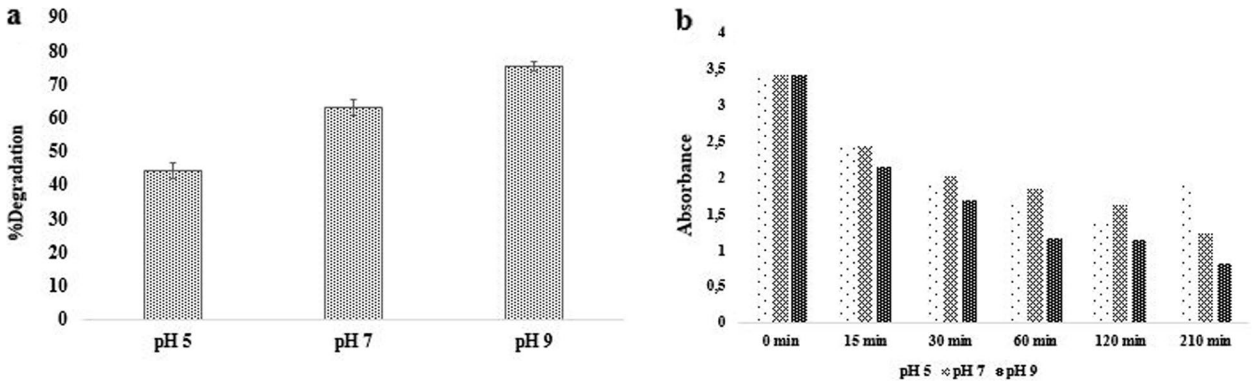

Fig. 7 Dye degradation activity of Cu@SSS hNFs against methylene blue. **a** degradation%, **b** time-dependent absorbance change

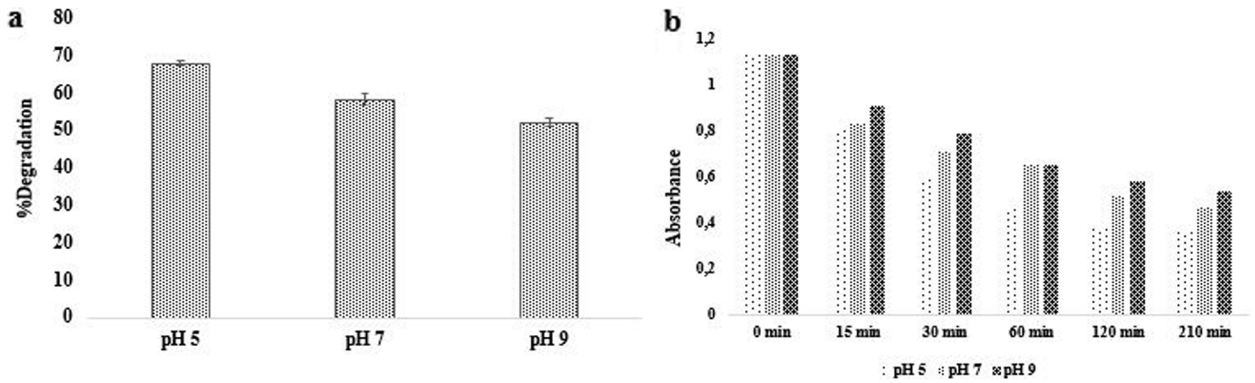

Fig. 8 Dye degradation activity of Cu@SSS hNFs against brilliant blue. **a** degradation%, **b** time-dependent absorbance change

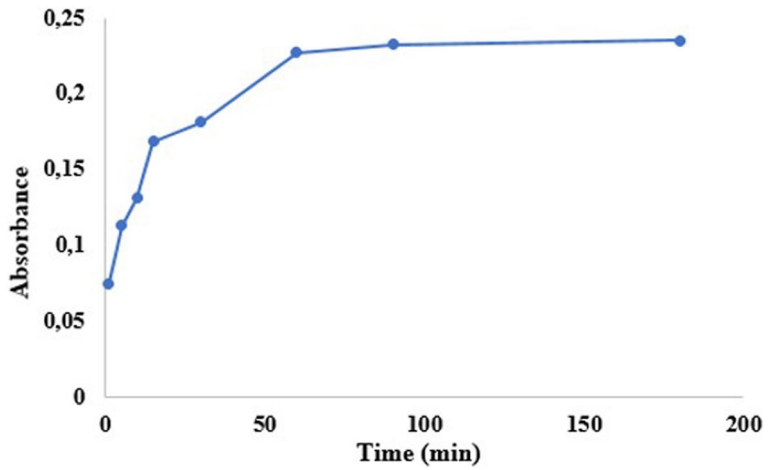

Fig. 9 The catalytic activity of Cu@SSS hNFs to guaiacol

according to the groups was compared using one-way analysis of variance. The Duncan test was used as a multiple comparison test. The $p<0.05$ value was considered statistically significant.

Discussion

Characterization of Cu@SSS hNFs

Details of the synthesis mechanism of hNFs in PBS buffer have been explained in previous studies [21, 27]

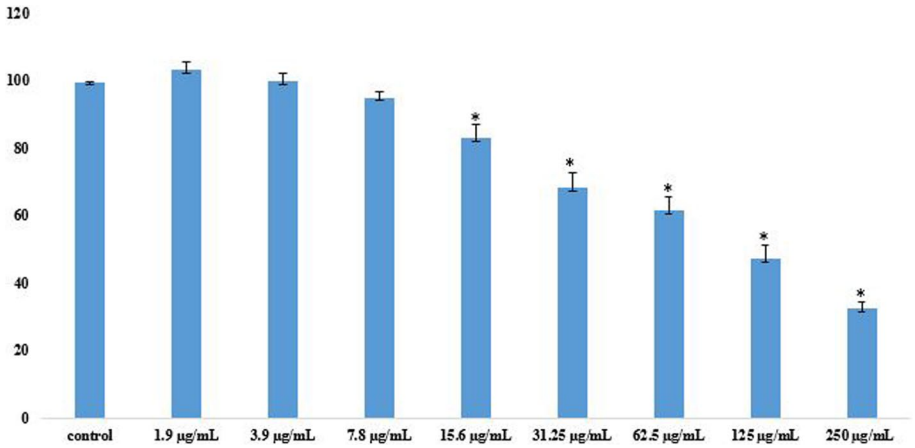

Fig. 10 Anticancer activity of Cu@SSS hNFs

and the introduction part of of this article. In the nucleation phase, where the synthesis begins, metal-phosphate crystals ($Cu_3(PO_4)_2$) are produced by the coordination of the phosphate groups (PO_4^{3-}) originating from the PBS buffer and the Cu^{+2} (bivalent metal) inorganic component. The metal-phosphate crystals formed bind to the reactive groups (amine, diol) of the organic component. During the growth phase, the coordination of metal-phosphate crystals and SSS extract (organic ingredient) continues, petals forming hNFs are formed, and these petals are connected to each other by the organic component acting as a glue. As hierarchical growth reaches the saturation phase, hNF synthesis is completed. In the three-step synthesis process of hNFs, the pH of the PBS where the synthesis takes place and the concentration of inorganic and organic ingredients are critical factors in this coordination reactionas they affect the synthesis of hNFs and the formation of their morphology. In the acidic PBS buffer, the organic component-$Cu_3(PO_4)_2$ coordination weakens due to the repulsion force between the protonated organic component and Cu^{+2}. This coordination reaction occurs through the nucleation zone of the organic component. The low concentration of organic components provides a low concentration of nucleation sites in the reaction medium and causes the synthesis of hNFs with different morphologies [23, 36]. With the presence of high concentrations of organic components, it is thought that (i) metal-extract complex structures are formed and the growth phase of hNFs is prevented [37], (ii) excess extract not involved in the coordination reaction blocks the pores of hNFs and disrupts their morphology [38]. However, it has been reported that when organic components are not used in the synthesis, only primary phosphate crystals are formed and no hNFs are formed as a result of the coordination of Cu^{+2} with phosphate from PBS buffer [39, 40]. In previous studies, consistent with our studies, it has been declared that acidity/alkalinity of medium, and concentration of organic components have notable effects on successful synthesis and morphological characteristics of hNFs.

The existence of Cu and other elemental components (O, C, N, and P) in the content of *Cu* hNFs synthesized through SSS as an organic component was shown by EDX analysis. The weight percentage of O, C, N, P, and Cu in the flower-shaped hybrid nanostructures are given as 30.57, 47.95, 3.55, 3.76, and 6.94, respectively. In addition, the atomic percentage values of flower-shaped hybrid nanostructures were determined as 28.62, 59.8, 3.79, 1.82, and 1.64, respectively. By XRD analysis, $2\theta = 9°$, 13°, 18°, 20°, 24°, 30°, 34°, 37°, 41.52°, 45°, 54°, and 56° correspond to $Cu_3(PO_4)_2$ and consist with JCPDS Card 00–022 –0548 [20, 25, 26]. Structural organic components of hNFs were revealed by using FT-IR diagrams. Amine groups (N–H) were associated with the peaks observed at wavelengths of 2926 and 1146 cm^{-1}. The entity of aromatic bond (C=C) was signed by absorbance observed at 1621 cm^{-1}. Other peaks (1034–558 cm^{-1}) observed in the FT-IR diagram match phosphate groups (P–O, P=O, PO_4^{-3}). However, data obtained from FT-IR analysis of SSS extract indicate that SSS extract contains amine and diol groups and therefore can coordinate with Cu^{+2}. In our study, the presence of Cu and amine in EDX and FT-IR analyses of hNFs is compatible with the synthesis mechanism of hNFs.

Antioxidant activity of Cu@SSS hNFs

Antioxidants have been proven to be helpful therapeutic and preventive agents and try to minimize this damage by dealing with oxidative impairment caused by reactive oxygen or free radical species [41]. It has been reported

that antioxidants reduce and clean DPPH as a result of their reaction with DPPH by releasing hydrogen [42]. According to this study, hNFs synthesized by hybridization of SSS and Cu^{+2} have concentration-dependent DPPH scavenging activity. It has been determined that the scavenging activity of safranal-based hNFs against DPPH depends on the medium pH and concentration [28]. The IC_{50} value of *Oxalis corniculata* leaf extract-based Zn NFs against DPPH was determined at 14.72 mg/ml [43]. Kiani et al. (2024) reported that the DPPH scavenging activity of Ag-doped ZnO NPs synthesized with Lavandula stoechas extract increased with the concentration increase from 250 µg/ml to 2000 µg/ml [9]. The DPPH scavenging activity of AgNPs synthesized with Petroselinum crispum extract increased from 47 to 96% with the concentration increase of Ag NPs from 31.25 µg/ml to 250 µg/ml [10]. Consistent with our data, previous studies have declared that the antioxidant activities of nanomaterials depend on concentration, consistent with our data [35, 44, 45].

Catalytic activity of Cu@SSS hNFs: degradation of methylene blue, brilliant blue, and guaiacol

According to our catalytic activity findings, SSS coordinated Cu hNF degraded methylene blue in the highest alkaline and lowest acidic medium. It has been noted that previously synthesized CuO-ZnO nanocomposites degrade methylene blue dye the lowest in an acidic medium and the highest in an alkaline medium [46]. Similar to our results, ZnO nanoparticles synthesized with curcumin extract adsorbed three different cationic dyes in the highest alkaline medium [47]. In Khan and coworkers' (2024) study, it was revealed that the crystal violet dye was highly degraded by citrate silver nanoparticles in a basic reaction solution [48]. It has been documented that under alkaline conditions, negatively charged hNFs might attract cationic dyes more effectively [46–48]. Our findings from the catalytic study are compatible with the literature showing that hNFs degrade methylene blue at a high rate in an alkaline medium. The weak catalytic activity exhibited by hNFs in the acidic medium in our study is explained by the repulsion force occurring between the protonation of hNFs and the cationic dye. The highest catalytic degradation of brilliant blue by hNFs in an acidic medium might be explained by the fact that positively charged hNF attracts the negatively charged anionic brilliant blue. Additionally, in our catalytic test, measurements of absorbance changes occurring with the oxidation of guaiacol were recorded. It is thought that hNFs cause the oxidation of guaiacol and transform it into 3,3-dimethoxy-4,4-diphenoquinone [49]. Consistent with relevant literature, we determined that Cu@SSS hNFs can oxidize guaiacol with peroxidase-like activity [26, 28, 30, 35].

In previous studies, the enhanced activities exhibited by hNFs were associated with their surface width, porosity, and 3D morphology [49, 50]. The catalytic performance of hNFs against substrates such as guaiacol and dyes has been mentioned via the Fenton oxidation process [21, 23, 30].

$$Cu^{2+} + H_2O_2 \rightarrow Cu^{+} + HOO^{0} + H^{+} \quad (1)$$

$$Cu^{+} + H_2O_2 \rightarrow Cu^{+2} + HO^{0} + H^{+} \quad (2)$$

Free radicals generated due to the reaction between Cu and H_2O_2 cause catalytic degradation by breaking down the model substrate.

Antimicrobial activity of Cu@SSS hNFs

We declare that hNFs exhibit effective antibacterial activity towards Gram (+) and Gram (-) strains with MIC values of 60 and 30 µg/ml. The MIC values of Lavandula stoechas extract-based Ag@ZnO NPs against *E. coli* and *S. aureus* strains were determined as 62.5 and 250 µg/ml, respectively [9]. MIC values of *Petroselinum crispum* extract-based Ag NPs against *E. coli and S. aureus* strains were measured as 31.25 and 125 µg/ml, respectively [10]. Hashemi et al., (2023a) reported that Ag NPs synthesized with different plant extracts exhibited different levels of antimicrobial activity [2]. The MIC value of *Axinyssa digitata* and Cu^{+2} directed synthesized hNFs was 32 µg/ml against examined two strains [51]. Demirbaş et al., (2023b) calculated the MIC of *Usnea antarctica*-coordinated Cu-based hNFs towards *E.coli* at 125 µg/ml, while it was determined at 62.5 µg/ml against *S. aureus* µg/ml [30]. In another study, the antimicrobial effect of cherry stalk-based Cu hNFs against *E. coli* was recorded at 2.5 mg/ml [35]. Researchers have associated the antibacterial activities of hNFs with the Fenton mechanism. Free radicals formed after the reaction cause oxidative damage to the bacterial cell wall and provide antimicrobial properties [52].

Anticancer activity of Cu@SSS hNFs

According to the data we obtained from the study, Cu@SSS hNFs exhibit anticancer activity against the A549 cell line. Somtürk Yılmaz et al., (2024) examined the anticancer activities of Co, Zn, and Cu hNFs synthesized via *Tribulus terrestris* against lung cancer (A549) cell lines [27]. Researchers reported that Co and Cu hNFs synthesized with *T. terrestris* extract coordination showed the highest and lowest anticancer activity against A549 cell lines, respectively. In a study evaluating the toxicity of hNFs, it was emphasized that the

Persea americana-directed Cu hNFs had more cytotoxicity to mouse fibroblast cells compared to the Zn hNFs synthesized with the same extract [53]. International Standard Organization (ISO 10993–5) considers a decrease in cell viability of more than 30% within the framework of cytotoxicity. According to our data, a statistically significant decrease in A549 viability was detected at 15.6 µg/ml exposure. Additionally, Cu hNFs reduced the cell viability below 70% at 31.25 and higher concentrations. Gwon et al., (2021) reported that Si@NiOOH nanoflowers had low cytotoxicity against mouse embryonic fibroblasts [54]. Shinde et al., (2020) determined that TiO2 nanoflowers have time-dependent cytotoxicity against HepG2 cell lines [55]. The toxicity caused by hNFs might be attributed to the fact that Cu^{+2} released from the structure of hNFs causes oxidative damage. If the cellular defense mechanism, consisting of enzymatic and non-enzymatic defense systems, cannot cope with oxidative stress, biomolecules are damaged and apoptosis occurs [55].

Conclusion

In the present study, SSS, an organic waste, was used to obtain hNFs by hybridization of organic and inorganic inputs. Using biological waste instead of enzymes and amino acids as organic components provides a cost advantage. The coordination ability of Cu^{+2} with the amine groups contained in the proteins found in snakeskin enabled the synthesis of hNFs. The pH of the PBS buffer affects the interaction of the primary phosphate crystals with the organic component by affecting the molecular charge of the organic components. Therefore, the synthesis of hNFs was synthesized depending on the pH of the medium. It has been noted that Cu@SSS hNFs display concentration-dependent antioxidant properties. In addition, the catalytic and antimicrobial activities exhibited by hNFs have been associated with the Fenton mechanism. According to this mechanism, free radicals formed after the reaction caused the degradation of the substrate. The cytotoxic effect of hNFs against the A549 cell line has been demonstrated. It is thought that hNFs synthesized with SSS extract can be used in anticancer, antioxidant, antimicrobial, and environmental technologies.

Acknowledgements
We would like to thank the Proofreading & Editing Office of the Dean for Research at Erciyes University for copyediting and proofreading service for this manuscript.

Authors' contributions
Cagri Caglar Sinmez: Planning of the study, Identification of snake, antioxidant and catalytic activities of nanoflowers. Fatih Doğan KOCA: Planning of the study, Methodology, Synthesis and characterization of Nanoflower, Writing.

Funding
Open access funding provided by the Scientific and Technological Research Council of Türkiye (TÜBİTAK).

Data availability
No datasets were generated or analysed during the current study.

Declarations

Ethics approval and consent to participate
Not applicable.

Consent for publication
Applicable.

Competing interests
The authors declare no competing interests.

Received: 13 June 2024 Accepted: 30 October 2024
Published online: 03 January 2025

References

1. Nejati M, et al. Synthesis of novel nano-radiotracer for in-vivo molecular SPECT imaging: Nanosize chitosan and its conjugation with glutamine. Arab J Chem. 2023;16: 105284.
2. Hashemi Z, et al. Anticancer and antibacterial activity against clinical pathogenic multi-drug resistant bacteria using biosynthesized silver nanoparticles with Mentha pulegium and Crocus caspius extracts. Inorg Chem Commun. 2023a;154:110982.
3. Ebrahimi A, et al. 99mTc- Anionic dendrimer targeted vascular endothelial growth factor as a novel nano-radiotracer for in-vivo breast cancer imaging. Bioorg Chem. 2022;128: 106085.
4. Sabouri Z, et al. Green Synthesis of Ag-Se doped ZnO-Co3O4-NiO fivenary nanocomposite using poly anionic cellulose and evaluation of their anticancer and photocatalyst applications. Chem Methodol. 2024;8(3):164–76.
5. Sabouri Z, et al. Biosynthesis of Ag doped MgO-NiO-ZnO nanocomposite with Ocimum Basilicum L extract and assessment of their biological and photocatalytic applications. J Mol Struct. 2024;1306: 137895.
6. Vijayakumar N, et al. Green synthesis of zinc oxide nanoparticles using Anoectochilus elatus, and their biomedical applications. Saudi J Biol Sci. 2021;29:2270–9.
7. Al-Radadi N. Laboratory scale medicinal plants mediated green synthesis of biocompatible nanomaterials and their versatile biomedical applications. Saudi J Biol Sci. 2022;29:3848–70.
8. Narm TS, et al. Biosynthesis of Se-doped ZnO/Ag2O/Fe3O4 nanocomposite using Sclerorhachis Leptoclada extract: Characterization and investigation of their photocatalytic effects. Environ Techno Inno. 2017;34: 103617.
9. Kiani Z, et al. Harmonizing nature and nanotechnology: Phytoextract-mediated synthesis of Ag-doped ZnO nanoparticles using Lavandula stoechas extract for environmental and biomedical applications. J Drug Deliv Sci Technol. 2024;96: 105708.
10. Zare-Bidaki M, et al. Enhanced in vivo wound healing efficacy and excellent antibacterial, antifungal, antioxidant and anticancer activities via AgNPs@PCS. Arab J Chem. 2023;16: 105194.
11. Hashemi Z, et al. In-vitro anticancer and antibacterial activities and comparative of eco-friendly synthesized silver nanoparticles using hull of Pistacia vera and rhizome of Sambucus ebulus extracts. Inorg Chem Commun. 2023b;154:110913.
12. Mohammadi-Aghdam S, Bahraini F, Ghoreishi SM. In-vitro anticancer on acute lymphoblastic leukemia NALM-6 cell line, antibacterial and catalytic performance of eco-friendly synthesized ZnO and Ag-doped ZnO nanoparticles using Hedera colchica extract. Biomass Convers Biorefin. 2024;14:20037–52.
13. Barzegarparay F et al. Green synthesis of novel selenium nanoparticles using Crataegus monogyna extract (SeNPs@CM) and investigation of its toxicity,

antioxidant capacity, and anticancer activity against MCF-7 as a breast cancer cell line. 2023, in press, https://doi.org/10.1007/s13399-023-04604-z.
14. Sahin M, Gubbuk IH. Green synthesis of palladium nanoparticles and investigation of their catalytic activity for methylene blue, methyl orange and rhodamine B degradation by sodium borohydride. React Kinet Mech Catal. 2022;135:999–1010.
15. Habib U, Ahmad Khan A, Rahman TU, Zeb MA, Liaqat W. Green synthesis, characterization, and antibacterial activity of silver nanoparticles using stem extract of Zanthoxylum armatum. Microsc Res Tech. 2022;85(12):3830–7.
16. Mostafavi M, et al. Hyperactivation of lipases by immobilization on superhydrophobic graphene quantum dots inorganic hybrid nanoflower. Int J Biol Macromol. 2024;254: 127817.
17. Rafiq A, Imran M, Aqeel M, Naz M, Ikram M, Ali S. Study of Transition Metal Ion Doped CdS Nanoparticles for Removal of Dye from Textile Wastewater. J Inorg Organomet Polym. 2020;30:1915–23.
18. Ikram M, et al. Experimental and computational study of annealed nickel sulfide quantum dots for catalytic and antibacterial activity. Nano Mater Sci. 2024;6:355–64.
19. Saadabadi RH, et al. Biosynthesis of ZnO-CeO2-Ag2O nanocomposite with Ocimum basilicum L seed extract as a highly efficient photocatalyst and assessment of their anticancer effects. Inorg Chem Commun. 2024;168: 112955.
20. Ge J, Lei J, Zare RN. Protein–inorganic hybrid nanoflowers. Nature Nanotech. 2012;7:428–32.
21. Demirbaş A, Karslı B, Ocsoy I. Facile synthesis of hybrid nanoflowers using glycine and phenylalanine and ınvestigation of their catalytic activity. Chem Biodivers. 2023a;20(8):e202300743.
22. Chen H, et al. A self-assembled 3D nanoflowers based nano-ELISA platform for the sensitive detection of pyridaben. Food Chem. 2024;445: 138756.
23. Koshy DS, et al. Silk Industry Waste Protein-Derived Sericin Hybrid Nanoflowers for Antibiotics Remediation via Circular Economy. ACS Omega. 2024;9:15768–80.
24. Tran TD, Nguyen PT, Le TN, Kim MI. DNA-copper hybrid nanoflowers as efficient laccase mimics for colorimetric detection of phenolic compounds in paper microfluidic devices. Biosens Bioelectron. 2021;182: 113187.
25. Koca FD, Muhy HM, Halici MG. Synthesis of hybrid Cu nanoflowers by using Tornabea scutellifera lichen extract, and evaluation of their dye degredation, and antioxidant activities. S Afr J Bot. 2023;160:394–401.
26. Koca FD, et al. Green synthesis of allicin based hybrid nanoflowers with evaluation of their catalytic and antimicrobial activities. Biotechnol Lett. 2020;42:1683–90.
27. Somtürk Yılmaz B, et al. Determination of anticancer activity and biosynthesis of Cu, Zn, and Co hybrid nanoflowers with Tribulus terrestris L. extract. Process Biochemistry. 2024;138:14–22.
28. Baldemir Kılıç A, Ildız N, Yusufbeyoğlu S, Öçsoy I. Nanoflower synthesis formed at different pH based on Crocus sativus L. (Croci stigma, saffron) extract and its major components: a new approach for enhancing antioxidant, antimicrobial and catalytic activities. Inorg Nano-Met Chem. 2023:1–11: https://doi.org/10.1080/24701556.2023.2240757.
29. Konuklugil B, Uras IS, Karsli B, Demirbas A. Parazoanthus axinellae extract incorporated hybrid nanostructure and its potential antimicrobial activity. Chem Biodivers. 2023;9: e202300744.
30. Demirbas A, et al. Formation of Umbilicaria decussata (Antarctic and Türkiye) extracts based nanoflowers with their peroxidase mimic, dye degradation and antimicrobial properties. Chem Biodivers. 2023b;20(8):e202300090.
31. Uras IS, Karsli B, Konuklugil B, Ocsoy I, Demirbas A. Organic–inorganic nanocomposites of Aspergillus terreus extract and ıts compounds with antimicrobial properties. Sustainability. 2023;15:4638.
32. Altinkaynak C, Kocazorbaz E, Özdemir N, Zihnioglu F. Egg white hybrid nanoflower (EW-hNF) with biomimetic polyphenol oxidase reactivity: Synthesis, characterization and potential use in decolorization of synthetic dyes. Int J Biol Macromol. 2018;109:205–11.
33. Jablonski D, et al. A new, rare, small-ranged, and endangered mountain snake of the genus *Elaphe* from the Southern Levant. Sci Rep. 2023;13:4839.
34. Sinmez CC, et al. Investigation of immunomodulatory and cytotoxic effects of shed snake skin (Elaphe sauromates) extract. Front Pharmacol. 2024;15: 1270970.
35. Güven OC, Kar M, Koca FD. Synthesis of cherry stalk extract based organic@inorganic hybrid nanoflowers as a novel fenton reagent: Evaluation of their antioxidant, catalytic, and antimicrobial activities. J Inorg Organomet Polym. 2022;32:1026–32.
36. Altinkaynak C, et al. Influence of Metal Ions and Organic Solutions on Activity and Stability of Beta-Glucosidase Nanoflowers. ChemistrySelect. 2024;9: e202304315.
37. Ildiz N, et al. Self assembled snowball-like hybrid nanostructures comprising Viburnum opulus L. extract and metal ions for antimicrobial and catalytic applications. Enzyme Microb Tech. 2017;102:60–6.
38. Altınkaynak C, et al. Synthesis of organic-inorganic hybrid nanoflowers using Trigonella foenum-graecum seed extract and investigation of their antimicrobial activity. Derim. 2019;36(2):159–67.
39. Jafari-Nodoushan et al. Organic-inorganic hybrid nanoflowers: The known, the unknown, and the future. Adv Colloid Interfac. 2022;102780.
40. Subramani G, et al. Organic-ınorganic hybrid nanoflower production and analytical utilization: fundamental to cutting-edge technologies. Crit Rev Anal Chem. 2022;52:1488–510.
41. Egbujor MC, et al. Phenothiazines: Nrf2 activation and antioxidant effects. J Biochem Mol Toxicol. 2024;38(3): e23661.
42. Gharehbeglou P, Sarabandi K, Akbarbaglu Z. Insights into enzymatic hydrolysis: Exploring effects on antioxidant and functional properties of bioactive peptides from chlorella proteins. J Agric Food Res. 2024;16: 101129.
43. Badgujar HF, Bora S, Kumar U. Eco-benevolent synthesis of ZnO nanoflowers using Oxalis corniculata leaf extract for potential antimicrobial application in agriculture and cosmeceutical. Biocatal Agric Biotechnol. 2021;38: 102216.
44. Prem P, et al. Valeriana jatamansi root extract a potent source for biosynthesis of silver nanoparticles and their biomedical applications, and photocatalytic decomposition. Green Chem Lett Rev. 2024;17:2305142.
45. Worku LA, Tadesse MG, Bachheti RK, Bachheti A, Husen A. Synthesis of carboxylated cellulose nanocrystal/ZnO nanohybrids using Oxytenanthera abyssinica cellulose and zinc nitrate hexahydrate for radical scavenging, photocatalytic, and antibacterial activities. Int J Biol Macromol. 2024;267: 131228.
46. Mardikar SP, Kulkarni S, Adhyapak PV. Sunlight driven highly efficient degradation of methylene blue by CuO-ZnO nanoflowers. J Environ Chem Eng. 2020;8(2): 102788.
47. Arab C, El Kurdi R, Patra D. Effect of pH on the removal of anionic and cationic dyes using zinc curcumin oxide nanoparticles as adsorbent. Mater Chem Phys. 2022;277:125504.
48. Khan A, Raza ZA, Bhatti HN, Sarwar T. Citrate silver nanoparticles impregnated cellulose as a photocatalytic filter in the degradation of organic dye in the aqueous media. Int J Biol Macromol. 2024;261:129881.
49. Somtürk B, Hancer M, Ocsoy I, Özdemir N. Synthesis of copper ion incorporated horseradish peroxidase-based hybrid nanoflowers for enhanced catalytic activity and stability. Dalton Trans. 2015;44:13845–52.
50. Yu X, et al. Regulated synthesis of 3D nano-flower-like MnCo2O4.5 catalytic materials to enhance thermal decomposition of ammonium perchlorate. Surf. Interfaces. 2024;46:104117.
51. Karsli B, Uras IS, Konuklugil B, Demirbas A. Synthesis of Axinyssa digitata extract directed hybrid nanoflower and investigation of its antimicrobial activity. IEEE T Nanobiosci. 2023;22:523–8.
52. Erdem T, Koca FD. Catalytic and antimicrobial activities of cucumber leaf extract-based organic@inorganic hybrid nanoflowers through Fenton-like reaction. Rend Lincei Sci Fish. 2023;34:1255–61.
53. Bor E et al. Synthesis of Persea americana extract based hybrid nanofowers as a new strategy to enhance hyaluronidase and gelatinase inhibitory activity and the evaluation of their toxicity potential. Inorg Nano-Met Chem. 2022; 1–13. https://doi.org/10.1080/24701556.2022.2072342.
54. Gwon K, et al. Highly bioactive and low cytotoxic Si-based NiOOH nanoflowers targeted against various bacteria, including MRSA, and their potential antibacterial mechanism. J Ind Eng Chem. 2021;99:264–70.
55. Shinde PV, Gagare S, Rout CS, Late DJ. TiO2 nanoflowers based humidity sensor and cytotoxic activity. RSC Adv. 2020;10:29378–84.

Publisher's Note